Supporting Information

Environmental Copper Sensor Based on Polyethyleneimine-Functionalized Nanoporous Anodic Alumina Interferometers

Simarpreet Kaur[1], Cheryl Suwen Law[2,3,4], Nathan Hu Williamson[1,5], Ivan Kempson[1*], Amirali Popat[6], Tushar Kumeria[6*] and Abel Santos[2,3,4*]

[1]Future Industries Institute, University of South Australia, Mawson Lakes, South Australia 5095, Australia.
[2]School of Chemical Engineering, The University of Adelaide, South Australia 5005, Australia.
[3]Institute for Photonics and Advanced Sensing, The University of Adelaide, South Australia 5005, Australia.
[4]ARC Centre of Excellence for Nanoscale BioPhotonics, The University of Adelaide, South Australia 5005, Australia.
[5]Eunice Kennedy Shriver National Institute of Child Health and Human Development, National Institutes of Health, Bethesda, Maryland, USA.
[6]School of Pharmacy, The University of Queensland, PACE Building, Queensland 4012, Australia.

***E-Mails:** ivan.kempson@unisa.edu.au ; t.kumeria@uq.edu.au ; abel.santos@adelaide.edu.au

Table of Contents

S-1. Optical Set-Up for Copper Binding by RIfS in Nanoporous Anodic Alumina Interferometers

RIfS spectra were measured using a miniature optical fiber spectrophotometer (USB 4000, Ocean Optics, USA) combined with a transparent flow cell based on acrylic plastic to create a microfluidics continuous flow system. The RIfS system is composed of a bifurcated optical probe, in which one of the arms carries white light from the tungsten source (LS-1LL, Ocean optics, USA). The optical probe illuminates white light onto the NAA sensing platform over a spot size of ~2 mm in diameter. Subsequently, the reflected light is collected by the other arm (i.e. collection fiber integrated into the same optical probe), which is guided to the miniature spectrophotometer. RIfS spectra were acquired over a wavelength range of 400–1000 nm and saved at intervals of 30 s, with an integration time of 10 ms and 50 average measurements. Changes in the effective optical thickness (ΔOT_{eff}) of NAA interferometers upon exposure to copper ions solutions were used as the sensing parameter in this study. All the stages of the process, including adsorption and crosslinking of PEI with GA as well as binding of Cu^{2+} ions onto PEI-GA-PEI-functionalized NAA interferometers, were monitored in real-time using this RIfS system. **Figure S1** shows the real-time monitoring of ΔOT_{eff} upon exposure to [Cu^{2+}] = 1–100 ppm solution.

S-2. Optimization of Working Parameters in Nanoporous Anodic Alumina Interferometers

Effect of Molecular Weight on Dynamic Binding of Cu^{2+} to PEI-GA-PEI Functional Layers

The amount of copper binding as a function of three molecular weights of PEI functional layers (i.e. 1300, 25000 and 750000 g mol^{-1}) in PEI-GA-PEI-modified NAA interferometers was investigated (**Figure 3a**). The flow rate of the analytical solution was kept constant at 100 µL min^{-1} and the surface chemistry architecture of NAA interferometers was functionalized with GA-crosslinked PEI molecules following the protocol described in Section 2.3. From the graph shown in **Figure 3a** it is apparent that ΔOT_{eff} increases with the molecular weight of the PEI molecules, with $\Delta OT_{eff\text{-}1300}$ = 3.9 ± 0.5 nm, $\Delta OT_{eff\text{-}25000}$ = 84.1 ± 2.2 nm and $\Delta OT_{eff\text{-}750000}$ = 174.8 ± 0.3 nm for PEI functional layers of 1300, 25000 and 750000 g mol^{-1} respectively. The degrees of branching (DB) of the three types of PEI measured by ^{13}C NMR spectroscopy were DB_{1300} = 0.63, DB_{25000} = 0.63, and DB_{750000} = 0.65 (**Figure S4**). PEI molecules of higher molecular weight provide more available ligand sites to capture Cu^{2+} ions present in the analytical solution. As a result, more ions are immobilized onto the inner surface of NAA interferometers, leading to more significant red shifts in ΔOT_{eff} (i.e. higher sensitivity). Therefore, further experiments were performed using PEI layers of 750000 g mol^{-1} molecular weight crosslinked with GA to maximize the sensing performance of the system.

Effect of Flow Rate on Dynamic Binding of Cu^{2+} to PEI-GA-PEI Functional Layers

Another critical factor affecting the dynamic binding of Cu^{2+} ions to PEI functional layers is the flow rate (R_{Flow}) of the analytical solutions through the flow cell system. To investigate the effect of this working parameter on the sensing performance of PEI-GA-PEI-functionalized NAA interferometers, we studied the binding of Cu^{2+} ions (i.e. 100 ppm) at four different flow rates (i.e. R_{Flow} = 50, 100, 200 and 300 μL min^{-1}). Changes in the effective optical thickness were used as a reference to establish the optimal flow rate; determined to be 100 μL min^{-1} (**Figure 3b)**. ΔOT_{eff} increases from 50 to 100 μL min^{-1} and decreases sharply when the flow rate is increased to 200 and 300 μL min^{-1} (i.e. $\Delta OT_{eff\text{-}50}$ = 126.1 ± 0.6 nm, $\Delta OT_{eff\text{-}100}$ = 174.8 ± 0.3 nm, $\Delta OT_{eff\text{-}200}$ = 23.4 ± 0.6 nm and $\Delta OT_{eff\text{-}300}$ = 25.8 ± 0.3 nm). This result can be attributed to the optimum residence time and the diffusion of copper ions into the sensing platform (**Figure 3b – left**). Excessive flow rates reduce the residence time of copper ions and limit their diffusion within the nanopores, minimizing the frequency of interactions between Cu^{2+} ions and the ligand sites present in the PEI-GA-PEI functional layers. As a result, the effective optical thickness change decreases dramatically beyond the optimal flow rate. Therefore, to maximize the sensing performance of our RIfS system, the flow rate was set to 100 μL min^{-1} throughout the set of experiments performed in this study.

Effect of Surface Chemistry on Dynamic Binding of Cu^{2+} to PEI-GA-PEI Functional Layers

Different PEI surface chemistries can be created at the inner interface of NAA interferometers. To discern the effect of this working parameter on the sensing performance of our system, we assessed the effective optical thickness changes associated with two different PEI chemistries, i.e. with (PEI-GA-PEI) and without (PEI-GA) a second PEI layer. Note that the rest of working parameters (i.e. PEI molecular weight and flow rate) were set to the optimal conditions (i.e. 750000 g mol^{-1} and 100 μL min^{-1}, respectively). **Figure 3c** shows the obtained results, which demonstrate that the amount of copper binding onto the PEI-GA-PEI films was significantly enhanced upon adsorption of a second layer of PEI after GA crosslinking of the primary PEI layer (i.e. $\Delta OT_{eff\text{-}PEI\text{-}GA}$ = 50.2 ± 0.5 nm and $\Delta OT_{eff\text{-}PEI\text{-}GA\text{-}PEI}$ = 174.8 ± 0.3 nm). A sandwiched PEI-GA-PEI surface chemistry increases the number of available chelating sites to bind Cu^{2+} ions present in the inner surface of the NAA interferometers, leading to more significant red shifts in the ΔOT_{eff} of the photonic films (i.e. ~3.5 times increased sensitivity).

S-3. Chemical Characterization via X-Ray Photoelectron Spectroscopy

The Cu/N atomic ratios in the PEI-GA-PEI-functionalized NAA interferometers after exposure to different copper concentrations were analyzed by XPS to establish the linear calibration range of the sensor (**Figure S3a**). XPS measurements were performed using the monochromatized Al Kα-rays (1486.7 eV) at a power of 225 W on a Kratos Axis-Ultra spectrometer (160 eV analyzer pass energy for survey scans, 20 eV for high-resolution scans) and an analysis spot size of ~300x700 μm. Core electron binding energies were given relative to a hydrocarbon C 1s binding energy of 284.8 eV. The data processing (i.e. peak fitting) and copper quantification were performed with the casa XPS software, using a Shirley-type background subtraction. The Cu/N ratio of the PEI-GA-PEI-modified NAA interferometers was determined as an average of analysis per spot for duplicates.

S-4. Distribution of Cu^{2+} in PEI-GA-PEI-Functionalized NAA Interferometers by Time-of-Flight Secondary Ion Mass Spectrometry (ToF-SIMS)

The spatial distribution of copper in PEI-GA-PEI-modified NAA interferometers was resolved across the nanopore cross-section of a ~12 μm NAA interferometer using a Physical Electronics Inc. PHI TRIFT V nanoTOF instrument (Physical Electronics Inc., Chanhassen, MN, USA) equipped with a pulsed liquid metal Au^+ primary ion gun (LMIG), operating at 30kV energy. Dual charge neutralization was provided by an electron flood gun (10 eV electrons) and 10 eV Ar^+ ions. Experiments were performed under a vacuum of $5x10^{-6}$ Pa. The spatial resolution was optimized using "Unbunched" Au_1 instrumental settings for the collection of images. All the chemical maps of species of interest were produced with images processed using WincadenceN software (Physical Electronics Inc., Chanhassen, MN, USA).

These observations are in good agreement with the results obtained for the calibration of ΔOT_{eff} vs $[Cu^{2+}]$ provided by our RIfS system, where ΔOT_{eff} increases linearly with $[Cu^{2+}]$. A PEI-GA-PEI-functionalized NAA interferometric platform exposed to 75 mg L^{-1} (i.e. 75 ppm) Cu^{2+} solution was cleaved for the purpose of assessing the polymer and Cu distribution in the cross-section (depth) of the sensing platform. ToF-SIMS was utilized to image various elemental and molecular fragments (**Figures S3b and c**). PEI, represented by a $C_2H_6N^+$ fragment, was observed as a band penetrating roughly 12 μm into the NAA interferometer. Correlating with the PEI distribution was a copper-based molecular fragment, $CuCH_3N^+$, consistent with a Schiff-base complex. The high degree of overlap between the Cu- and PEI-based fragments suggests a uniform distribution of PEI-associated Cu, confirming the successful and selective binding of copper ions by the PEI-GA-PEI functional layers.

S-5. Characterization of PEI Branching by ^{13}C NMR

The level of branching of PEI molecules for each molecular weight was measured by ^{13}C NMR, following the protocol established by Holycross and Chai.[S1] Solutions of PEI were prepared at 10 wt % in Milli-Q water and transferred to 5 mm NMR sample tubes. The experiments were performed using a 300.13 MHz (^{1}H frequency) Avance II NMR spectrometer (Bruker BioSpin, Germany) equipped with a broadband multinuclear solutions probe (PABBO) and 5 mm radio frequency coil. 1-D ^{13}C NMR spectra were acquired at 75.468 MHz with inverse gated decoupling, 240 ppm sweep width, 1024 scans, and 5 µs RF pulse length (~30° tip angle) (**Figure S4**). The repetition time (TR) was set to 5 s after first testing that ratios of the integrated peak intensities were the same as with a 20 s TR. Fourier transforms with 1 Hz line broadening, baseline subtraction, and peak integrations were performed in Topspin 2.1.

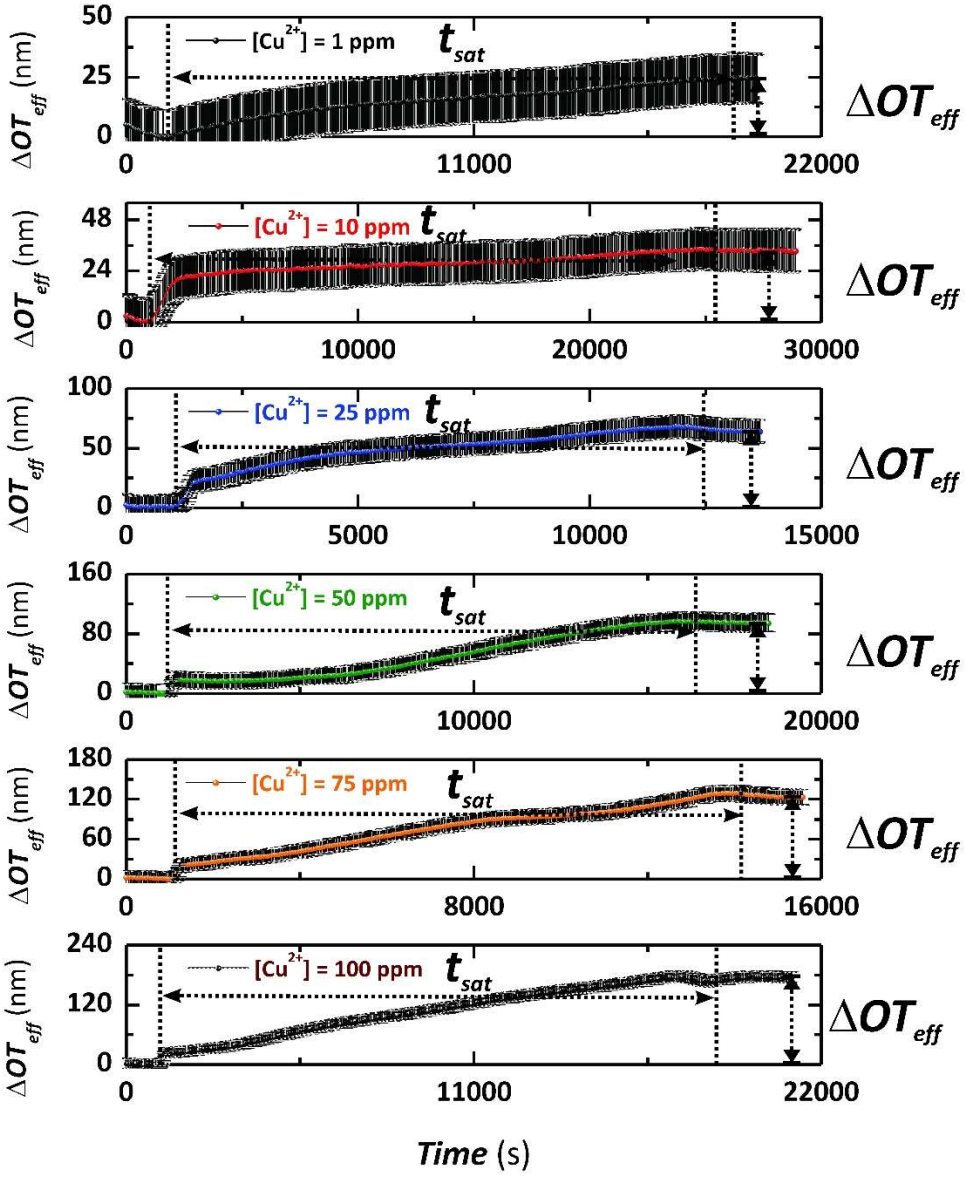

Figure S1. Real-time Cu^{2+} binding stage for [Cu^{2+}] = 1–100 ppm, where the arrows indicate ΔOT_{eff} and t_{sat} for the binding reaction performed under dynamic flow conditions (note: the dotted line shown at the left of the graphs indicates the timepoint at which the Cu^{2+} analytical solutions were injected into the flow cell system – OT_{eff} and time baselines).

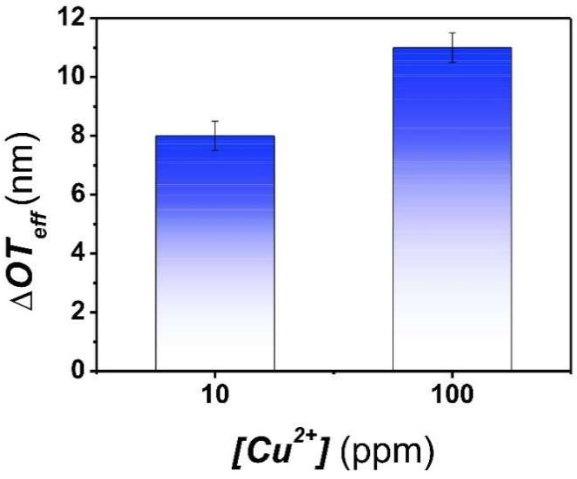

Figure S2. Changes in effective optical thickness (ΔOT_{eff}) of non-functionalized NAA interferometers upon exposure to analytical solutions of copper ions of $[Cu^{2+}]$ = 10 and 100 ppm.

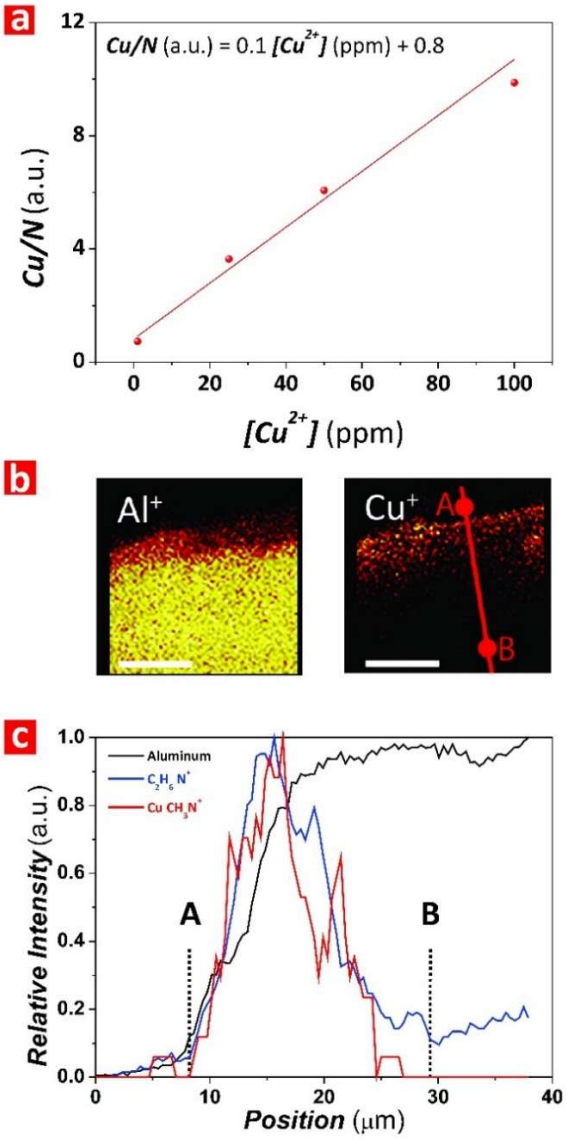

Figure S3. Validation of chemistry interaction between PEI-GA-PEI functional layers and copper ions in functionalized NAA interferometers. a) Linear correlation between Cu/N ratio and $[Cu^{2+}]$ quantified by XPS in PEI-GA-PEI-functionalized NAA interferometers upon exposure to 1, 25, 50 and 100 mg L^{-1} Cu^{2+} analytical solutions. b) Cross-sectional elemental and molecular distributions by ToF-SIMS analysis, where Cu penetration into a NAA interferometer upon exposure indicates a uniform association of Cu with PEI to a depth of approximately 12 μm. Images of Al^+ and Cu^+ are shown with an artificial color map, with black being lowest and white the greatest intensities respectively (scale bar = 10 μm). c) A linescan indicated by the red line in the Cu^+ image shown in (b) provides the profile presented in the plot (note: data for the molecular fragments have been smoothed by plotting a 5-point moving average).

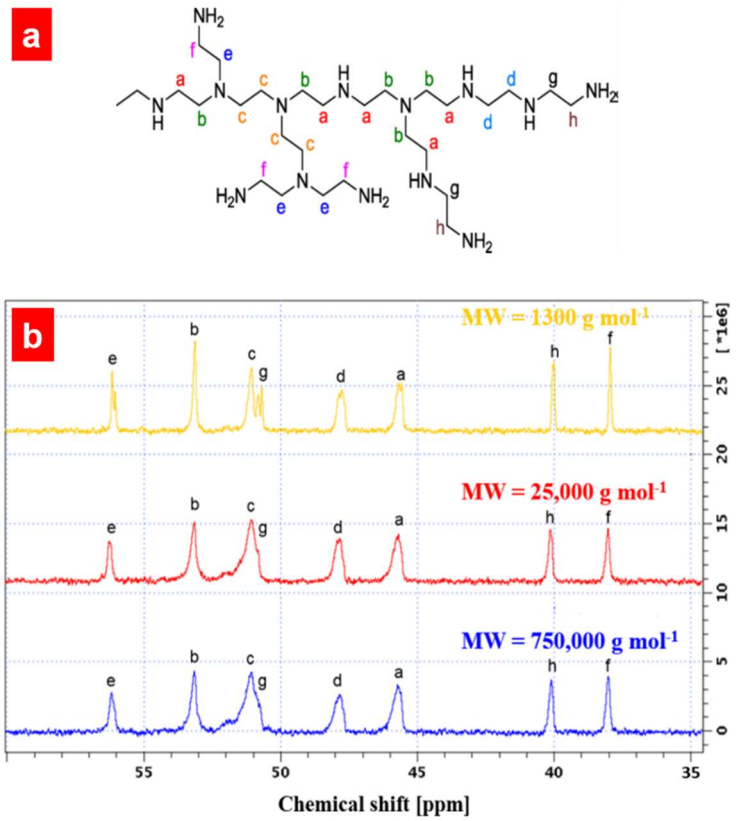

Figure S4. a) Chain fragment of branched PEI with labels indicating carbons (methylene groups) with different chemical environments uniquely defined by the types of amino groups in the ethyleneimine unit.[S1] b) ^{13}C NMR spectra of the three types of PEI. Integrals under the peaks were used to measure the degrees of branching, as defined by DB = (1° +3°)/(1° +2°+3°)[S1] where 1°,2°, and 3° are primary, secondary, and tertiary amines, with the first and second ^{13}C peak from each type of amine providing a unique signal.[S2]

Table S1. Metal concentration in centrifuged solution of acid mine drainage liquid at pH 5, as determined through ICP-OES. Errors indicate ± min/max (n=2).

Metal	**Al**	**Cd**	**Cu**	**Fe**	**Ni**	**Pb**	**Zn**
[M] (mg/L)	134.4 ± 0.6	< 0.005	30.8	532 ± 1	0.55	< 0.005	21.4

REFERENCES

[S1] Holycross, D.R.; Chai. M., Comprehensive NMR Studies of the Structures and Properties of PEI Polymers. *Macromolecules* **2013**, *46*, 6891-6897.
[S2] Hawker, C.J.; Lee, R.; Fréchet, J.M.J., One-Step Synthesis of Hyperbranched Dendritic Polyesters. *J. Am. Chem. Soc.* **1991**, *113*, 4583-4588.